Binodal and spinodal curves: A simulation for various high polymer mixtures

D. J. Walsh and S. Rostami
Department of Chemical Engineering and Chemical Technology, Imperial College of Science and Technology, London S. W. 7., UK
(Received 31 May 1984; revised 10 September 1984)

Flory's equation-of-state theory has been used to predict the lower critical solution temperature behaviour of polymer–polymer mixtures. The spinodal phase boundary of numbers of high molecular weight polymer mixtures have been previously simulated using this theory. In this paper a procedure for simultaneous predictions of the binodal and the spinodal curves by equating the chemical potential of each component in the mixture is presented. The method is tested for five different mixtures. The effects of the binary and pure component state parameters on the simulated curves are discussed and the simulated phase diagrams are compared with the experimental cloud point curves. It is found that in most cases the results are more consistent with the cloud point curve being closer to the spinodal curve than the binodal.

(Keywords: polymer miscibility; polymer compatibility; polymer phase diagrams; polymer blends)

INTRODUCTION

High molecular weight polymers, when miscible, are often found to phase separate on heating, showing lower critical solution temperature (*LCST*) behaviour. The binodal is the curve connecting the compositions of co-existing phases and is defined by:

$$(\Delta\mu_1)_A=(\Delta\mu_1)_B \qquad (\Delta\mu_2)_A=(\Delta\mu_2)_B \tag{1}$$

where $(\Delta\mu_i)_A$ and $(\Delta\mu_i)_B$ are the chemical potentials of component i at two points A and B on the binodal at equilibrium relative to their standard states. Above the binodal is a region of metastability. The spinodal is the limit of this metastable region and is defined by:

$$\frac{d(\Delta\mu_i)}{d\phi_2}=0 \tag{2}$$

where ϕ_2 is the segment fraction of component 2. The binodal and the spinodal meet at the critical point where

$$d^2(\Delta\mu_i)d\phi_2^2=0 \tag{3}$$

Various theoretical treatments have been used to describe and predict the phase diagrams. The Flory–Huggins lattice theory in its simplest form is unable to predict *LCST* behaviour. Various modifications to the lattice theory have introduced lattice site vacancies to take account of volume changes on mixing and/or empirical temperature and composition dependent interaction terms. These have often been able to describe the phase behaviour without always giving a great deal of insight into the processes involved. These theories have been described and reviewed elsewhere[1,2].

The theory which has extensively been applied to the phase diagrams of high-molecular-weight polymer mixtures is the equation-of-state theory of Flory and co-workers[3,4]. McMaster used this theory to calculate the spinodals and the binodals of hypothetical polymer mixtures[5]. He examined the contribution of the pure and binary state parameters and showed that the theory is capable of predicting both *LCST* and upper critical solution temperature (*UCST*) behaviour individually or simultaneously. Olabisi applied this treatment to simulate the spinodal curves of a real system, poly(caprolactone) and poly(vinyl chloride)[6]. We have used a modified form of the above theory to simulate the spinodal curves of mixtures of poly(methyl methacrylate) with chlorinated polyethylene[7], poly(butyl acrylate) with chlorinated polyethylene[8], ethylene–vinyl acetate copolymers with chlorinated polyethylene[9], and poly(ethylene oxide) with polyether sulphone[10].

In this paper we describe the simulation of the binodal curves for the above polymer mixtures. These can be compared to the simulated spinodal curves and the measured cloud points which must lie between the binodal and the spinodal.

THEORY

With the notation of Flory and his collaborator[3,4] as shown in the Appendix, the equation for the chemical potential of each component of the mixture can be derived. The equation-of-state of the pure components and of the mixture is given by

$$\tilde{P}\tilde{v}/\tilde{T}=\tilde{v}^{1/3}/(\tilde{v}^{1/3}-1)-1/\tilde{T}\tilde{v} \tag{4}$$

At atmospheric pressure this equation yields

$$\tilde{T}=(\tilde{v}^{1/3}-1)/\tilde{v}^{4/3} \tag{5}$$

Knowing the thermal expansion coefficients, α_i, and

0032-3861/85/030418-05$03.00
© 1985 Butterworth & Co. (Publishers) Ltd.

thermal pressure coefficients, γ_i, of the pure components, and using equation (5), it is possible to calculate the reduced volumes, $\tilde{v}_i$, hard core temperatures T_i^* and hard core pressures P_i^* from,

$$\tilde{v}_i^{1/3} = (3+4\alpha_i T)/(3+3\alpha_i T)$$
$$P_i^* = \gamma_i T \tilde{v}_i^2 \qquad (6)$$
$$\tilde{T}_i = T/T_i^*$$

One can then calculate the hard core pressure, P^*, and temperature, T^*, of the mixture from

$$P^* = \phi_1 P_1^* + \phi_2 P_2^* - \phi_1\theta_2 X_{12} \qquad (9)$$

$$\tilde{T} = T/T^* = (\phi_1 P_1 \tilde{T}_1 + \phi_2 P_2^* \tilde{T}_2)/P^* \qquad (10)$$

where X_{12} is the interaction parameter and can be obtained experimentally from, for example, heat of mixing measurements, and θ_2 is given by

$$\theta_2 = (S_2/S_1)\phi_2/((S_2/S_1)\phi_2 + \phi_1) \qquad (11)$$

where S_2/S_1 is the surface-area-to-unit-volume-ratio which can be obtained by a group contribution method[11]. From these values one can calculate the reduced volume of the mixture $\tilde{v}$ using equation (5).

The chemical potential of component 1 in the mixture is given by[7,9]

$$\Delta\mu_1 = RT[\ln\phi_1 + (1-r_1/r_2)\phi_2] + P_1^* V_1^* \{3\tilde{T}_1 \ln[(\tilde{v}_1^{1/3}-1)/(\tilde{v}^{1/3}-1)] + \tilde{v}_1^{-1} - \tilde{v}^{-1} + \tilde{P}_1(\tilde{v}-\tilde{v}_1)\} + (X_{12} - TQ_{12}\tilde{v})V_1^*\theta_2^2/\tilde{v} \qquad (12)$$

where Q_{12} is the non-combinatorial entropy correction which is generally used as an adjustable parameter. When subscripts 1 and 2 are interchanged one obtains an expression for the chemical potential of component 2. This can more usefully be expressed as

$$\Delta\mu_2 = RT[\ln\phi_2 + (1-T_2/r_1)\phi_1] + (P_2^* V_1^* r_2/r_1)\{3\tilde{T}_2 \ln[(\tilde{v}_2^{1/3}-1)/(\tilde{v}^{1/3}-1)] + v_2^{-1} - \tilde{v}^{-1} + \tilde{P}_2(\tilde{v}-\tilde{v}_2)\} + (X_{12} - TQ_{12}\tilde{v})V_1^*\theta_2^2 S_2 r_2/S_1 r_1 \tilde{v} \qquad (13)$$

Using equations (12) and (13) and the binodal condition, equation (1), one can thus compute the position of the binodal curve. This process involves a search procedure whereby positions of equal chemical potential of component 1 are found and one looks for the minimum difference between the chemical potentials of component 2 over these positions.

The equation for the spinodal is obtained by differentiating equation (12) and applying the spinodal condition, equation (2) to give[7,9]

$$1/\phi_1 + (1-T_1/r_2) - (P_1^* V_1^* D/RT_1^*)/(\tilde{v}-\tilde{v}^{2/3}) + (P_1^* V_1^* D/RT)(1/\tilde{v}^2 + \tilde{P}_1) + (V_1^* X_{12}/RT)[2\theta_1\theta_2^2/\tilde{v}\phi_1\phi_2) - (\theta_2^2 D/\tilde{v}^2)] - 2V_1^* Q_{12}\theta_1\theta_2^2/R\phi_1\phi_2 = 0 \qquad (14)$$

where

$$D = d\tilde{v}/d\phi_2$$

which can be calculated as described previously[7,9].

The spinodal equation can be solved directly or can alternatively be found from the maxima and minima of $\Delta\mu_i$ while carrying out the search procedure for the binodal, and these give identical results.

MATERIALS

The properties and state parameters of all the pure components of the mixtures discussed are shown in *Table 1*. How these values were obtained and the justification for the values used are given in previous papers in which the simulations of the spinodals were also described[7-10].

The molecular weights used were the weight averages and the effects of polydispersity were ignored. However,

Table 1 Properties of pure components

Material		$\bar{M}$ x 10^{-5} [a]	α x 10^{-4} (K^{-1})	γ ($Jcm^{-3}K^{-1}$)	v_{sp} (cm^3g^{-1})	Temperature at which data are given °C
Chlorinated polyethylene 52 w% Cl	CPE3	1.2	3.6546	0.9592 (0.9)	0.8089	83.5
Chlorinated polyethylene 43 w% Cl	H48	1.8	4.4199	0.9544	0.81506	83.5
Ethylene–Vinyl acetate copolymer 45 w% AC	EVA45	2.00	4.5103	0.8045	1.0636	83.5
Polyether sulphone	PES	0.2	2.0	1.5	0.7934	25.0
Poly(ethylene oxide)	PEO	0.2	5.5	1.2	0.9183	25.0
Poly(butyl acrylate)	PBA	1.2	5.47	1.556	0.9523	70.0
Chlorinated polyethylene						
50 w% Cl	CPE17	1.82	5.66	0.963	0.7502	70.0
51.6 w Cl	CPE16	1.98				
Poly(methyl methacrylate)	PMMA17	0.144	5.74	1.171	0.8333	30.0
	PMMA5	28.6				

[a] $\bar{M}_w$ by g.p.c. relative to polystyrene standards

Table 2 Binary state parameters of mixtures

Binary mixture	S_2/S_1	X_{12} (cm^{-3})	Q_{12} ($Jcm^{-3}K^{-1}$)	$\frac{r_1}{r^2}$
EVA45–CPE3	1.03	−3.2	−0.0063	2.86
		(−.603)	(0)	
EVA45–H48	0.98	−2.86	−0.00678	1.86
		(−0.5)	(−0.00138)	
PES/PEO	1.2	−40	−0.04	0.08
	(1.1)			
PBA–CPE17	1.02	−9.525	−0.02381	0.86
		(−1.0123)	(−0.00263)	
PMMA17–CPE16	1.064	−3.04	−0.00608	0.085
PMMA5–CPE16	1.064	−3.04	−0.00608	1.55

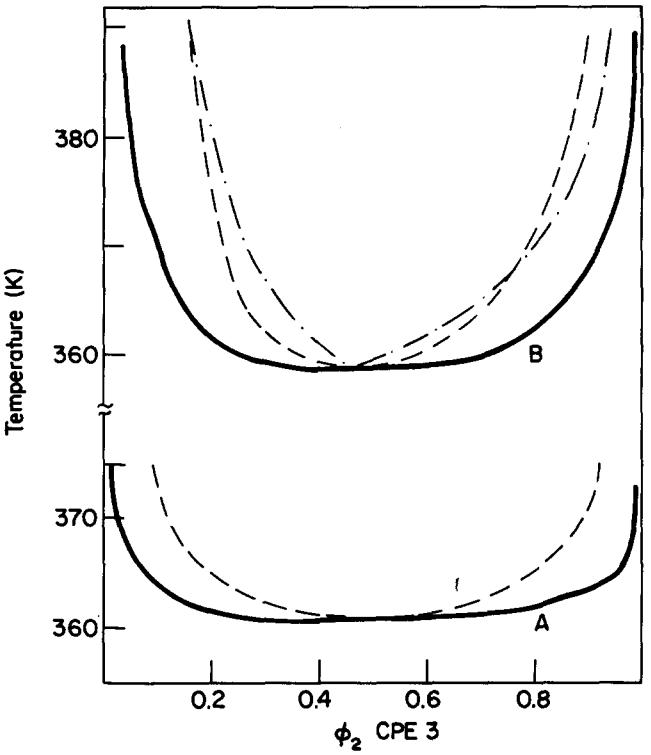

Figure 1 Simulated binodal (——) and spinodal (-----) curves for blends of EVA45 and CPE 3 using the data of *Tables 1* and *2* at the following conditions. Lower curves (A): x_{12}=3.2 Jcm^{-3} Q_{12}=-0.0063 $Jcm^{-3}K^{-1}$. Upper curves (B): x_{12}=−2.86 Jcm^{-3} Q_{12}=0 $Jcm^{-3}K^{-1}$, γ_2=0.9 $Jcm^{-3}K^{-1}$. The experimental cloud point curve[13] is also shown (- · - · -)

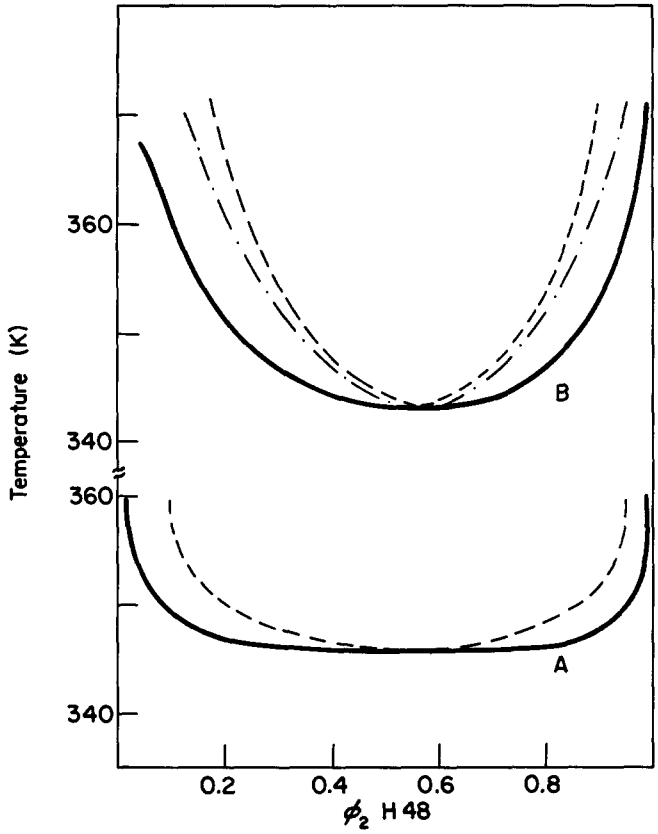

Figure 2 Simulated binodal (——) and spinodal (-----) curves of EVA45 and H48 mixtures using the data of *Tables 1* and *2* at the following conditions. Lower curves (A): x_{12}=−2.86 Jcm^{-3} Q_{12}=−0.00678 $Jcm^{-3}K^{-1}$. Upper curves (B): x_{12}=−0.5 Jcm^{-3}, Q_{12}=−0.00138 $Jcm^{-3}K^{-1}$. The experimental cloud point curve of the mixture[13] (—·—·—) is also shown for comparison

for high molecular weight polymers having large favourable interaction parameters the combinational terms in the free energy expression are relatively small and thus the effects of polydispersity should also be small.

The binary state parameters of the mixtures from the same sources are shown in *Table 2*. The values of the interactional parameter, X_{12}, were all obtained from heat of mixing measurements on low molecular weight analogues. The Q_{12} values were adjusted to fit the simulated spinodals to the cloud point curves at their minima. Where second values for any of the parameters are shown in brackets, these values were adjusted values used in the simulation of spinodals in order to make them consistent with the measured cloud point curves. In some cases, for example, the simulated spinodals were very flat and lay outside the cloud point curve, an impossible situation. Smaller values of X_{12} were then chosen (with appropriate smaller Q_{12} values) to locate the spinodal close to the cloud point.

RESULTS AND DISCUSSION

Poly(ethylene-co-vinyl acetate) EVA45)/chlorinated polyethylene (52% Cl; CPE3)

The simulated spinodal and binodal curves for mixtures of EVA45 and CPE3 were calculated using the data shown in *Tables 1* and *2* and the results are shown in *Figure 1*. The initial curves (A) are very flat bottomed. This is probably due to the fact that the value of X_{12} obtained from the heats of mixing of low molecular weight analogues is higher than that of the actual polymers or that X_{12} may be temperature dependent. A second set of curves (B) has been calculated with a lower value of X_{12} (adjusted to require $Q_{12}=0$) and a slightly adjusted value for γ_2. The cloud point curve is also given for comparison in the Figure[13]. Using these values the spinodal can be made to fit fairly closely to the cloud point curve. It is also

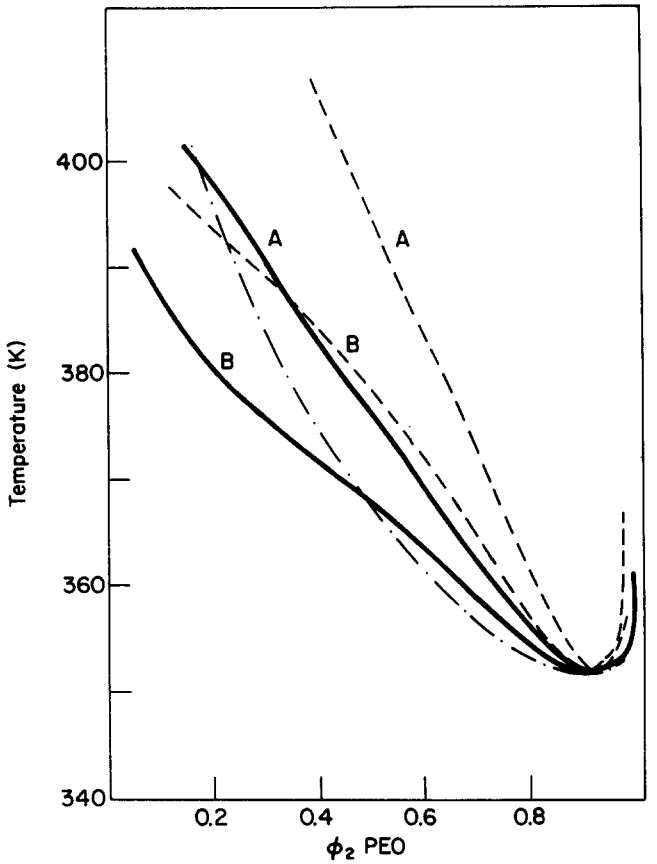

Figure 3 Simulated binodal (——) and spinodal (-----) curves of PES/PEO mixtures using the data of *Tables 1* and *2*. The values of S_2/S_1 ratio used for each simulation. The curves in (A) = 1.2 and the curves in (B) = 1.1. The experimental cloud point curve of the mixture[10] is also shown (-·-·-)

found that no reasonable values of any of the parameters can easily be found which can make the calculated binodal curve fit to the measured cloud point. This suggests that the cloud point must be closer to the spinodal than the binodal curve which is not surprising considering the slow rates of phase separation which might be expected for such high molecular weight polymers.

Poly(ethylene-co-vinyl acetate) (EVA45)/chlorinated polyethylene (43% Cl; H48)

The spinodal and binodal curves for these polymer mixtures were simulated using the procedure described for the previous blends. The conclusions drawn are also similar. In *Figure 2* the initial phase diagram is very flat-bottomed and a lower value of $X_{12} = -0.5$ J cm^{-3} with $Q_{12} = 0.00138$ J cm^{-3} K^{-1}. This is a phase diagram which is more consistent with the experimental cloud points. Again no reasonable values of these parameters could be found to move the binodal curve close to the cloud points.

Polyether sulphone (PES)/Poly(ethylene oxide) (PEO)

The phase diagram as simulated for this system is shown in *Figure 3*. The experimental cloud point curve is also shown for comparison[10]. Using the initial data the cloud point curve falls below the spinodal and binodal curves, an impossible situation. Reducing the value of S_2/S_1 from a theoretical value of 1.2 to 1.1 lowers the phase diagram closer to the experimental cloud point curve. It should be noticed that this parameter affects the skew nature of the curves whereas adjusting χ_{12} and Q_{12} affects the curvature and the location but maintains the symmetry. However, since the terms in equations (12)–(14) containing X_{12} and Q_{12} are multiplied by θ_2, which depends on S_2/S_1, the relative sizes of these effects are interlinked.

It would at first sight appear that the data is more consistent with the cloud point curve being close to the binodal. This may be possible since the rate of diffusion in this system has been observed to be very high with the phase separation being reversible on annealing at temperatures below the cloud point. This could, however, also be due to uncertainties in the values of the various state parameters.

Poly(butyl acrylate) (PBA)/chlorinated polyethylene (50% Cl; CPE17)

The simulations of the spinodals for PBA/CPE17 mixtures have been reported earlier[8]. The binodal and spinodal curves, using the values of X_{12} and Q_{12} given in *Table 2* are shown in *Figure 4*. The phase diagram using an initial value of X_{12} shown by the lower set of curves is very flat-bottomed whereas that in the upper set of curves using a smaller negative X_{12} value is located closer to the experimental cloud point curve as shown by the dotted line. As in the case of EVA/CPE mixtures, it is not easy to find reasonable values of the parameters which can be used to adjust the binodal to fit the cloud point curve.

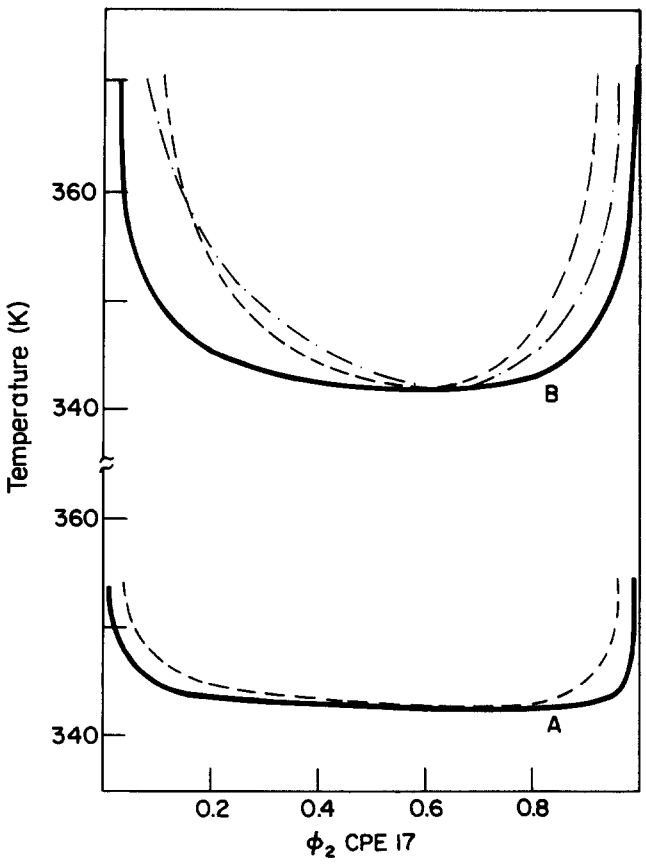

Figure 4 Simulated binodal (———) and spinodal (– – –) curves of PBA and CPE17 blends. The values of χ_{12} and Q_{12} used in these simulations are given below[8]. Lower curves (A): $\chi_{12} = -9.525$ Jcm^{-3}, $Q_{12} = -0.0238$ Jcm^{-3} K^{-1}. Upper curves (B): $\chi_{12} = -1.0123$ Jcm^{-3}, $Q_{12} = -0.0026$ Jcm^{-3} K^{-1}. The experimental cloud point curve of the mixture as reported earlier[8] is also shown (-·-·-)

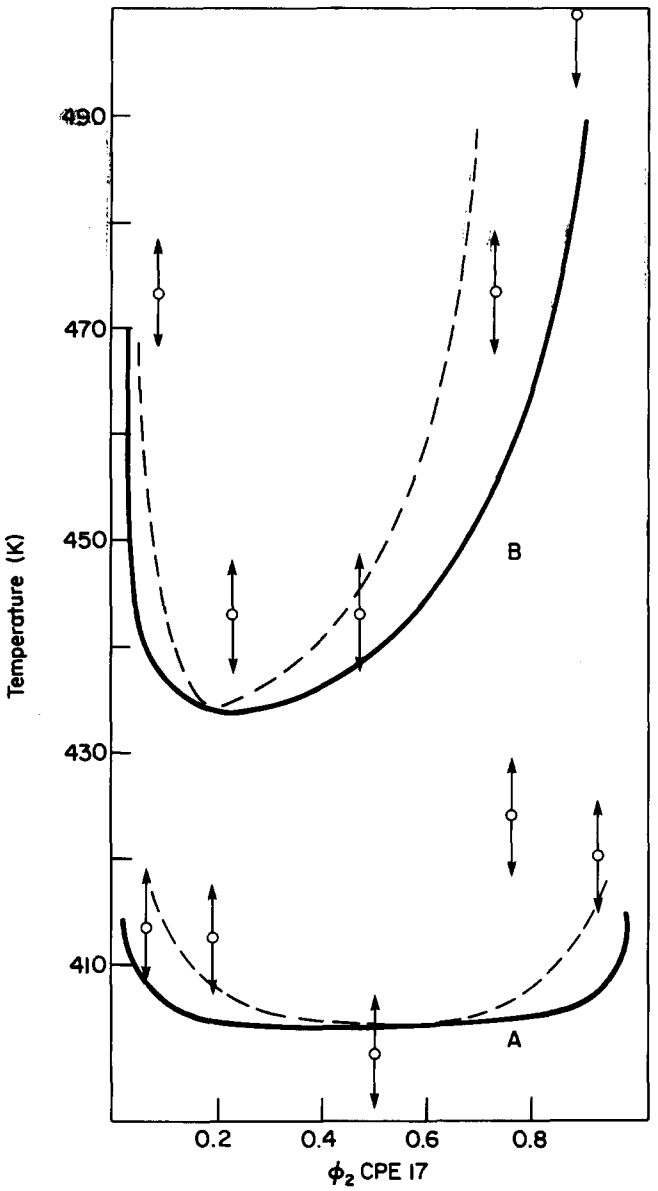

Figure 5 Simulated binodal (——) and spinodal (-----) curves of blends of CPE17 with PMMA of different molecular weights. The data of *Tables 1* and *2* were used for these simulations where in lower curves (A) the PMMA has molecular weight of 26.4×10^4 and in the upper curves (B) the PMMA has a molecular weight of 1.44×10^4, relative to standard polystyrene. The experimental cloud points are also shown in the Figure

Poly(methyl methacrylate) (PMMA)/chlorinated polyethylene (51.6% Cl; CPE16)

The simulated spinodal and binodal curves for mixtures of CPE16 with PMMA having different molecular weights are shown in *Figure 5*. The crude cloud point data, obtained by observing two glass transition temperatures after heating above the phase separation temperatures using a differential thermal analysis technique are also shown in the Figure. The accuracy of this technique is thought to be at best ± 5°C. Taking this into consideration the simulated curves follow the cloud point trends satisfactorily. They also demonstrate the effect of polymer molecular weight on the position and shape of the phase diagram.

CONCLUSIONS

The equation-of-state theory of Flory and co-workers can be used to simulate the *LCST* spinodal and binodal curves of high molecular weight polymer mixtures. In some cases this requires the non-combinatorial entropy correction, Q_{12}, to be used as an adjustable parameter.

In some systems the value of X_{12} calculated from heats of mixing of low molecular weight analogues appears to be over-estimated. This could be due to differences between the analogues and the polymers or due to a temperature dependence of X_{12}.

Generally the experimental cloud points are closer to the spinodal curve than to the binodal and in some cases no reasonable values of the various parameters can be chosen to fit the binodal to the cloud point curve. This might be expected since nucleation should not occur easily in high polymer mixtures. The one exception to this appears to be for PES/PEO mixtures where the cloud points lie closer to the binodal. This could be due to the very high diffusion rates in this system allowing nucleation to occur. It could also be due to uncertainties in the estimation of the state parameters, particularly to surface-area-to-unit-volume ratio S_2/S_1.

REFERENCES

1 Paul, D. R. and Newman, S. (Eds.) 'Polymer Blends', Academic Press, 1978
2 Olabisi, O., Robson, L. M. and Shaw, M. T. 'Polymer–Polymer Miscibility', Academic Press, New York (1979)
3 Flory, P. J., Orwell, R. A. and Vrij, A. *J. Am. Chem. Soc.* 1964, **86**, 3507
4 Flory, P. J. *J. Am. Chem. Soc.* 1965, **87**:9, 1833
5 McMaster, L. P. *Macromolecules* 1973, **6**, 760
6 Olabisi, O. *Macromolecules* 1975, **9**, 316
7 Chai, Z., Ruona, S., Walsh, D. J. and Higgins, J. S. *Polymer* 1983, **24**, 263
8 Chai, Z. and Walsh, D. J. *Makromol. Chem.* 1983, **184**, 1549
9 Rostami, S. and Walsh, D. J. *Macromolecules* 1984, **17**, 315
10 Walsh, D. J., Rostami, S. and Singh, V. B. *Makromol. Chem.* in press
11 Bondi, A. *J. Phys. Chem.* 1964, **68**, 441
12 Walsh, D. J., Rostami, S. *Adv. Polym. Sci.* in press
13 Walsh, D. J., Higgins, J. S. and Rostami, S. *Macromolecules* 1983, **16**, 387
14 Walsh, D. J. and Singh, V. B. *Makromol. Chem.* 1984, **185**, 1979

APPENDIX

P	pressure
$\tilde{P}_i$	reduced pressure of species i
P_i^*	hard core pressure of species i
$\tilde{P}$	reduced pressure of mixture
P^*	hard core pressure of mixture
Q_{12}	interaction entropy parameter
R	gas constant
r_i	chain length of molecule i
S_i	number of contact sites per segment in species i
T	temperature
$\tilde{T}_i$	reduced temperature of species i
T_i^*	hard core temperature of species i
$\tilde{T}$	reduced temperature of mixture
T^*	hard core temperature of mixture
V_i^*	molar hard core volume of component i
v_{sp}	specific volume of component i
$\tilde{v}_i$	reduced volume of component i
v_i^*	hard core volume of component i
$\tilde{v}$	reduced volume of mixture
v^*	hard core volume of mixture
X_{12}	interaction parameter
ϕ_i	segment fraction of species i
θ_i	site fraction of species i
$\Delta\mu_i$	chemical potential of component i